Article

Post-Closure Performance Assessment for Deep Borehole Disposal of Cs/Sr Capsules

Geoff A. Freeze *, Emily Stein and Patrick V. Brady

Sandia National Laboratories, Albuquerque, NM 87185, USA; ergiamb@sandia.gov (E.S.);
pvbrady@sandia.gov (P.V.B.)
* Correspondence: gafreez@sandia.gov

check for updates

Abstract: Post-closure performance assessment (PA) calculations suggest that deep borehole disposal of cesium (Cs)/strontium (Sr) capsules, a U.S. Department of Energy (DOE) waste form (WF), is safe, resulting in no releases to the biosphere over 10,000,000 years when the waste is placed in a 3–5 km deep waste disposal zone. The same is true when a hypothetical breach of a stuck waste package (WP) is assumed to occur at much shallower depths penetrated by through-going fractures. Cs and Sr retardation in the host rock is a key control over movement. Calculated borehole performance would be even stronger if credit was taken for the presence of the WP.

Keywords: boreholes; cesium (Cs); strontium (Sr)

1. Introduction

Deep borehole disposal (DBD) for the geologic isolation of spent nuclear fuel (SNF) and high-level radioactive waste (HLW) has been considered for many years, beginning with evaluations of nuclear waste disposal options by the National Academy of Sciences in 1957 [1]. Efforts by the United States and the international community over the last half-century toward the disposal of SNF and HLW (collectively referred to as high-activity waste) have primarily focused on mined geological repositories. Nonetheless, evaluations of DBD have periodically continued in several countries [2–6].

The DBD concept, illustrated in Figure 1, consists of drilling a large-diameter borehole into crystalline basement rock to a depth of about 5000 m, placing waste packages (WPs) in the lower, waste emplacement zone portion of the borehole, and sealing and plugging the upper portion of the borehole with a combination of bentonite, cement plugs, and sand/crushed rock backfill. Waste in a DBD system is several times deeper than typical mined repositories (e.g., Onkalo and waste isolation pilot plant (WIPP)) and is well below the typical maximum depth of fresh groundwater resources, as indicated by the dashed blue line in Figure 1. The characteristics and conditions of the DBD concept that favor the long-term isolation of radioactive waste from the accessible environment include the following.

- Great depth of disposal: DBD safety relies on emplacing wastes in competent crystalline rock well below the extent of naturally circulating groundwater. In DBD, waste would be situated at 3 to 5 km depth in low-permeability granite or schist, so the radionuclide migration path distance would be an order of magnitude greater than for mined repositories, which are typically proposed at depths of approximately 500 m.

- Isolation and long residence time of deep groundwater: recent studies have shown that groundwater deeper than 2 km in the Precambrian basement was isolated from the atmosphere for more than one billion years, e.g., [7,8]. The origin and residence time of deep groundwater can be estimated using environmental tracers with long half-lives (e.g., ^{36}Cl, ^{81}Kr, ^{4}He, ^{234}U/^{238}U ratio). In addition, deep groundwaters are typically concentrated chloride brines with densities

that range from 2.5% greater than pure water (seawater) to more than 30% greater than pure water [9,10]. High salinity at depth can be indicative of isolation from shallower water.
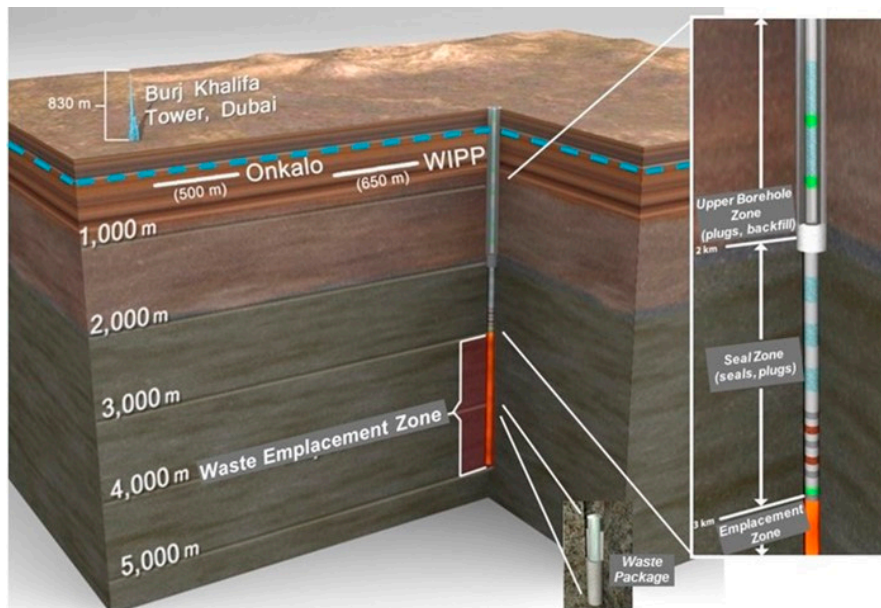

Figure 1. Generalized schematic of the deep borehole disposal (DBD) concept. WIPP: waste isolation pilot plant.

- Density stratification of brine at depth: the density stratification of brine tends to limit the effects from future perturbations to hydrologic conditions such as climate change, or from early thermal convection in the borehole due to heat production from radionuclide decay. The density gradient (fresh water near the surface, concentrated brine at depth) is stabilizing and inhibits vertical flow or mixing. The simple existence of concentrated chloride brines in the crystalline basement is a general indicator of great age, especially when no evaporites are present in the geologic setting. The absence of overpressured conditions at depth (so that in situ pressure cannot drive flow toward the surface) is also expected at favorable locations for DBD.
- Low permeability of crystalline host rock: the bulk permeability of deep crystalline rocks is generally low and decreases with depth.
- High likelihood of slow diffusion-dominated radionuclide transport: movement in groundwater is practically the only significant pathway for the migration of radionuclides from a deep borehole to the accessible environment. If the groundwater has not moved for millions of years (i.e., minimal advection due to low permeability and low regional hydraulic head gradient), then transport is limited to the mechanism of aqueous diffusion, which is a slow process.
- Geochemically-reducing conditions at depth: reducing conditions in the deep subsurface tend to limit the solubility and enhance the sorption of many radionuclides, further reducing mobility in groundwater.
- Low permeability and high sorption capacity of seal materials: the low permeability of seal materials (bentonite and cement) inhibits vertical fluid flux and radionuclide transport up the borehole; the high sorption capacity of the bentonite also limits and/or delays radionuclide transport, e.g., [5]. Seals are primarily needed during the first few hundred years of maximum decay heat production in the borehole. Further seal performance is desirable until the re-establishment of the natural salinity gradient (density stratification), which tends to oppose upward flow.
- Multi-barrier design: the safety of a DBD system includes contributions from natural barriers (deep, isolated low-permeability host rock) and engineered barriers (multiple, redundant sealing intervals and materials). Although not required for post-closure safety under currently analyzed

scenarios, longer-lived, engineered waste forms (WFs) and/or WPs would further contribute to waste isolation and multi-barrier capability.

Safe borehole disposal is possible at shallower depths, over a range of borehole diameters, depending on the target geologies and WFs. Viable options range from low-level waste and sealed sources in "shallow" boreholes (<hundreds of meters deep) to intermediate-level radioactive waste and HLW in "deeper" boreholes (<~2000 m). Depth to basement would be an important consideration. For these shallower borehole concepts, the demonstration of post-closure safety relies on a combination of engineered and natural system performance, similar to a mined repository; the reliance on the engineered seals may be greater.

2. Deep Borehole Disposal of Hanford Cs/Sr Capsules

Here, we emphasize the performance assessment (PA) of the "very deep" DBD concept, with waste emplacement at a depth of about 5000 m. The focus is on the disposal of smaller U.S. Department of Energy (DOE)-managed WFs, such as cesium (Cs) and strontium (Sr) capsules, which are less than 0.09 m (3.5 in) in diameter [11]. Shallower disposal of sealed sources containing short-lived radionuclides have been analyzed by Ojovan et al. [12] and International Atomic Energy Agency (IAEA) [13].

Subsurface features and components of the borehole and host rock, as shown in Figure 2, include: borehole and casing, WF, WP, emplacement zone (EZ) (buffer/backfill/annulus, cement plugs, liner), seal zone (SZ), and upper borehole zone (UBZ). The reference disposal concept includes a 5000-m deep borehole with a bottom-hole (i.e., EZ) diameter of 0.311 m (12.25 in). This design is expected to be achievable in crystalline rocks with currently available commercial drilling technology. We consider both the nominal case, where "everything goes as planned", and a disturbed "stuck package" where a WP gets permanently wedged in the borehole above the EZ near a hypothetical borehole-intersecting fracture.
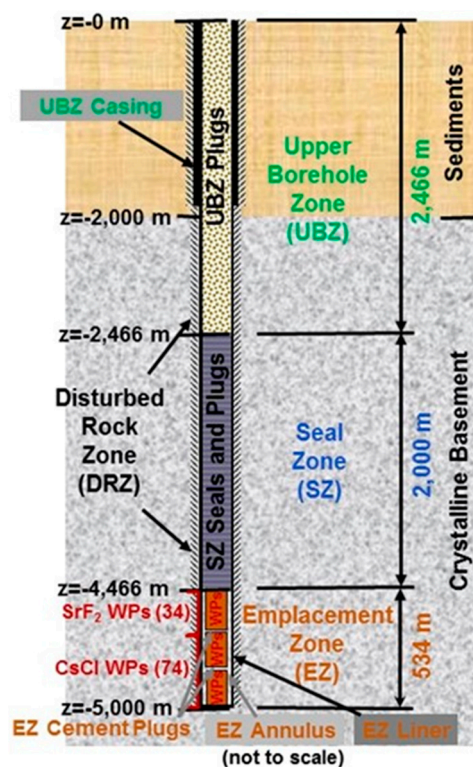

Figure 2. Schematic of the DBD concept for Cs/Sr capsules. Source: Freeze et al. [5].

The DOE-managed inventory of 1335 Cs capsules (containing glass-like CsCl, cooled from a molten pour) and 601 Sr capsules (containing granular, compacted SrF_2 precipitate, chiseled from drying pans) is currently stored at the Hanford Waste Encapsulation and Storage Facility, and are all less than 0.09 m (3.5 in) in diameter [11]. These capsules contain short-lived ^{90}Sr and ^{137}Cs, and long-lived ^{135}Cs; other radionuclides have decayed away.

The WPs containing the Cs and Sr capsules would be placed in the lower EZ portion of the borehole (between 4466 and 5000 m depth). Each carbon steel WP is assumed to contain 18 Cs or Sr capsules, stacked in six layers of three capsules (three-packs) each (Figure 3). Each WP would have an outside diameter of 0.219 m (8.625 in) and a total length of 4.76 m, which includes 3.76 m for the six layers of capsules, a 0.3-m long fishing neck (to facilitate retrieval during operations), and a 0.7-m-long impact limiter (to minimize damage from drops). With this reference design (other configurations are possible), 108 WPs would be required to accommodate all of the Cs/Sr capsules (74 for the Cs capsules and 34 for the Sr capsules), and all of the WPs would fit in a single borehole with an EZ that was 0.311 m (12.25 in) in diameter and 534-m long (this length includes 10-m long cement plugs above the 40th and 80th WPs for structural support).
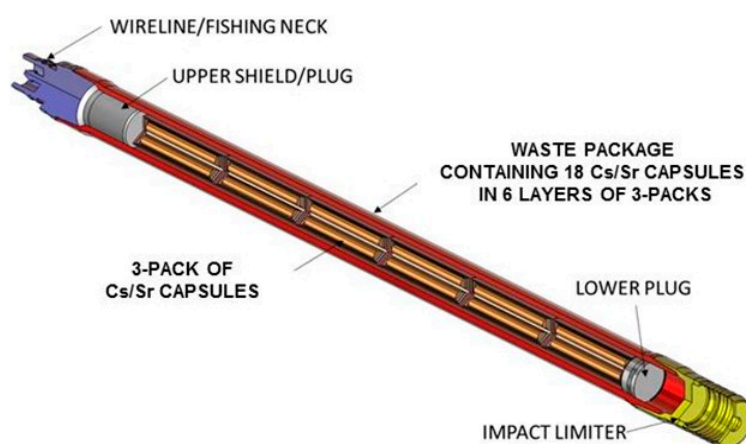

Figure 3. Schematic of a waste package (WP) for Cs/Sr capsules. Source: Freeze et al. [5].

A perforated steel liner is assumed to extend the length of the EZ. A temporary guidance casing from the surface will be designed to work in conjunction with the EZ liner to facilitate the smooth emplacement of WPs. The EZ also includes annular spaces between the stacked WPs and the EZ liner and between the EZ liner and the borehole wall. These annular spaces could be filled with buffer or backfill material. However, for the reference disposal concept, the EZ annular regions are assumed to be filled with high-density brine, similar to formation fluid.

The upper portion of the borehole includes the SZ, which is entirely within the crystalline basement rock, and where seals and plugs (bentonite seals, cement plugs, silica sand/crushed rock ballast) will be emplaced directly against borehole wall, and the UBZ, primarily within the sedimentary overburden, where plugs (cement alternating with ballast) will be emplaced against the cemented casing. The SZ is a 2000-m interval (between 2466 and 4466 m depth). Seals in the SZ are designed to act directly against the disturbed rock zone (DRZ) of the host rock to limit upward radionuclide transport; cement plugs in the SZ would minimize the chemical interaction between adjacent seals.

The nominal scenario for the DBD of Cs/Sr capsules was developed using a feature, event, and process (FEP) analysis and scenario development methodology [5]. The conceptual model was implemented using the geologic disposal safety assessment (GDSA) framework [14] for numerical simulations of thermal hydrology and radionuclide mobilization and transport in a high-performance computing environment. The GDSA framework includes PFLOTRAN [15], which is an open source, massively parallel non-isothermal multi-phase flow and reactive transport code, and DAKOTA

(http://dakota.sandia.gov/), which is an analysis package for uncertainty quantification, sensitivity analysis, optimization, and calibration in a parallel computing environment.

Key nominal scenario modeling assumptions are:

- Thermal output and radioactivity from the Cs and Sr capsules assumes surface storage/aging until borehole emplacement in 2050.
- WFs (solid CsCl and SrF$_2$) are assumed to degrade immediately after emplacement and do not perform any function (e.g., gradual dissolution) that would delay radionuclide release or transport. Unlimited solubility of Cs and Sr in groundwater is assumed.
- A 534-m EZ contains 108 WPs (74 for the Cs capsules and 34 for the Sr capsules). The cooler Cs WPs are emplaced first, in the lower portion of the EZ. The WPs are assumed to maintain structural integrity during surface handling and emplacement, but are assumed to degrade immediately after sealing (corresponding to a simulated WP breach time of one year after sealing) and do not perform any function (e.g., gradual corrosion) that would delay radionuclide release or transport.
- A 2000-m SZ has permeability and porosity that is consistent with degraded properties of bentonite clay, cement plugs, and/or sand/crushed rock ballast. The overlying UBZ also has permeability and porosity that is consistent with degraded material properties.
- Sparsely fractured crystalline basement rock has low permeability and porosity and no regional hydraulic head gradient.
- Overlying sediments are represented as a single vertically and laterally homogeneous region. This model simplification does not impact the results, because radionuclides are not transported beyond the crystalline basement rock in any of the simulations.
- A DRZ around the borehole is assumed to have an elevated permeability with respect to the adjacent intact basement rock due to the changes in stress induced by drilling.
- A temperature gradient with depth is calculated assuming a geothermal heat flux of 60 mW/m^2 at 6000-m depth and an average annual surface temperature of 10 °C. The resulting thermal gradient is ~25 °C/km, with ambient temperatures of about 125 °C at the top of the EZ and 140 °C at the bottom of the EZ.
- There is potential for advective and diffusive aqueous-phase transport. Radionuclide mobilization and transport properties are based on geochemically reducing conditions consistent with deep crystalline rock (consideration of the gas phase and/or colloidal transport is deferred to a future PA).

The material properties used to represent these DBD system features and processes in the nominal scenario PA simulations are summarized in Table 1. For the stuck package scenario (Figure 4), the following changes are made to the nominal scenario reference case:

- A single Cs WP is assumed to remain stuck in the crystalline basement above the EZ near a borehole-intersecting fracture. As a remedial measure, it is assumed that cement was injected (through the annulus outside the guidance casing) into the SZ below the stuck package. The injected cement is assumed to be more permeable and more porous than the engineered cement plugs. The specific properties of the injected cement are listed in Table 1.
- The properties of the borehole-intersecting fracture (Table 1) are derived from a porous medium representation of a discrete fracture (see Section 2.2 below). The fracture was assumed to have a 30° dip, intersecting the borehole at a depth of 2540 m (540 m below the base of sedimentary overburden). Two cases were analyzed: one with no regional hydraulic head gradient (as in the nominal scenario), and one with a regional hydraulic head gradient of 0.0001 m/m, driving flow up-dip toward the sediments.

Table 1. Numerical representation of material properties in the performance assessment (PA) simulations. DRZ: disturbed rock zone, EZ: emplacement zone; and WP: waste package.

Material	Permeability k (m^2)	Porosity ϕ (-)	Tortuosity τ (-)	Effective Diffusion Coeff. D_e [a] (m^2/s)	Thermal Cond. (W/m·K)	Heat Capacity (J/kg·K)	Bulk Density ρ_{rock} (kg/m^3)	Sr K_d [b] (L/kg)	Cs K_d [b] (L/kg)
Emplacement Zone									
WP	1×10^{-16}	0.43	1.0	4.30×10^{-10}	17	500	7850	0	0
EZ annulus (brine-filled)	1×10^{-12}	0.99	1.0	9.90×10^{-10}	0.58	4192	1100	0	0
Cement plug	1×10^{-18}	0.175	0.175	3.06×10^{-11}	1.7	900	2700	0	0
Injected cement [c]	1×10^{-16}	0.25	0.25	6.25×10^{-11}	1.7	900	2700	0	0
Seal Zone									
Cement plug	1×10^{-18}	0.175	0.175	3.06×10^{-11}	1.7	900	2700	0	0
Bentonite seal	1×10^{-18}	0.45	0.45	2.03×10^{-10}	1.3	800	2700	1525	560
Ballast	1×10^{-14}	0.20	0.20	4.00×10^{-11}	2.0	800	2700	0	0
Host Rock									
Crystalline rock	1×10^{-18}	0.005	0.20	1.00×10^{-12}	2.5	880	2700	1.7	22.5
DRZ	1×10^{-16}	0.005	0.20	1.00×10^{-12}	2.5	880	2700	1.7	22.5
Fracture [c]	1×10^{-14}	8.1×10^{-6}	123 [d]	1.00×10^{-12}	2.5	880	2700	1.7	22.5
Sediments									
Sediments	1×10^{-15}	0.20	0.20	4.00×10^{-11}	2.0	800	2700	50	120

[a] D_e = free water diffusion coefficient ($D_w = 1 \times 10^{-9}$ m^2/s) × tortuosity × porosity. [b] K_d = distribution coefficient (for linear sorption). [c] Stuck package scenario only. [d] Fracture tortuosity value that results in an appropriate effective diffusion coefficient.
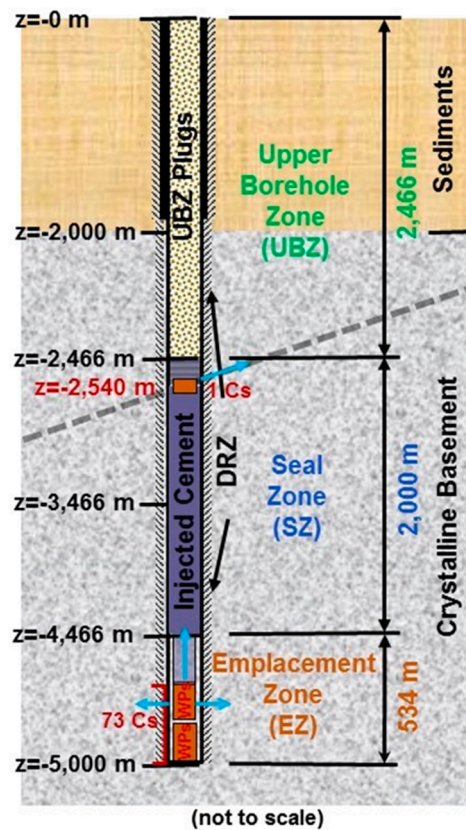
Figure 4. Schematic of the DBD stuck package scenario. Source: Freeze et al. [5].

2.1. Crystalline Basement Hydraulic Head Gradient

The groundwater flow rate is quantified by the Darcy velocity (also referred to as specific discharge), v_D (m/s) [16]:

$$v_D = K\,i \tag{1}$$

where:

　　K = hydraulic conductivity (m/s)
　　i = hydraulic (head) gradient (m/m)

and:

$$K = (k\,\rho\,g)/\mu \tag{2}$$

$$i = \Delta h/\Delta l \tag{3}$$

where:

　　k = permeability (m^2)
　　ρ = fluid density (kg/m^3)
　　g = gravitational constant (m/s^2)
　　μ = fluid viscosity (kg/m-s) = (Pa-s) = (cp)
　　Δh = head difference (m)
　　Δl = distance between head measurements (m)

The center-of-mass of a non-reactive solute (e.g., a non-sorbing dissolved radionuclide) moves in flowing groundwater at the groundwater pore velocity, v_x (m/s). The groundwater pore velocity (also referred to as average linear groundwater velocity) derives from the Darcy velocity and the porosity, ϕ:

$$v_x = v_D/\phi \tag{4}$$

The effects of sorption onto the porous medium can be quantified simplistically (i.e., assuming linear sorption) in terms of a retardation factor, R_f:

$$R_f = 1 + (\rho_{rock}\, K_d)/\phi \tag{5}$$

where:

ρ_{rock} = rock bulk density (kg/m^3)
K_d = distribution coefficient (L/g)

For non-reactive solutes, K_d is 0 and R_f is 1. For reactive solutes, K_d is >0 and R_f is >1. This leads to the definition of an apparent groundwater velocity, v_a (m/s), that represents the effective velocity of a sorbing radionuclide through the porous medium:

$$v_a = v_x/R_f \tag{6}$$

The distance, x (m), traveled by the center-of-mass of a solute (dissolved radionuclide) in time, t (s), is then:

$$x = v_a\, t \tag{7}$$

K_d's describing Sr and Cs uptake (Table 1) by solids are relatively high in bentonite clay, and lower in the rock matrix. Note also that the K_d model of adsorption is very simplistic, and that a more precise picture of contaminant transport might be gained using site-specific measurements and a more complex sorption model.

Data on groundwater flow rates and hydraulic heads and gradients in the deep crystalline basement are sparse, largely because the low permeability and poor water quality means that most of the drilling and resource exploration occurs in shallower units. Topographic relief is the dominant mechanism for groundwater flow in continental land masses, both in the shallow and deep subsurface. Maximum flow rates of 1 to 10 m/yr develop in deep aquifers, while much smaller seepage rates occur in aquitards [17]. In the dolomite strata of the Appalachian and Illinois basins in Missouri, minimum flow rates of 1 mm/yr occur in the deepest Cambrian shale [17]. In the Precambrian Shield in Canada, groundwater flow occurs through both the granitic and metamorphic bedrock and the overburden deposits. The near-surface bedrock (<400 m depth) has low primary hydraulic conductivity ($<10^{-10}$ m/s), but zones of localized, relatively high, secondary hydraulic conductivity (10^{-6} to 10^{-8} m/s) and low interconnected porosity (0.1 to 0.001) are associated with a rock-mass fracture system [18]. Flat-lying fracture zones, where present, are the major controls on regional flow. These zones have been encountered at various depths between the surface and at least 1000 m, with a generalized vertical spacing of 1 to 300 m and a thickness of 10 to 50 m [18]. Within these zones, permeability is highly anisotropic; distinct flow channels in the fracture plane are a controlling feature. The flat-lying fracture zones are associated with steep fault zones that penetrate to great depth and often appear as long lineaments at the surface. These zones also appear to be highly anisotropic, with permeability controlled by both fracture fillings and regional stresses. The spacing of these steep fault zones varies from less than l km to greater than 5 km.

Regional stresses are important in the hydraulic properties of these faults [18]. Where the maximum horizontal compressive stress is normal to the strike, these faults tend to be closed or tight and chemically filled. The opposite has been observed where regional stresses are parallel to the zone. A similar correlation of regional stress and permeability has been noted in work at the Stripa Mine in Sweden.

In the relatively intact rock blocks between major fault zones, the rock is tight. All the fractures are chemically filled and, except for the deep semi-horizontal zones of high permeability mentioned above, the groundwater flow is minimal, and no systematic flow pattern has been measured or observed [18].

Regional hydraulic head gradients in the order of 0.001 m/m have been reported in deep sedimentary aquifers [19–21]. Site investigations were performed at Forsmark and Oskarshamn in

Sweden in boreholes in fractured granite down to depths of about 1000 m. These site investigations yielded estimates of groundwater flow rates, transmissivities, and hydraulic head gradients [22]. Hydraulic gradients calculated from borehole flow rates, estimated transmissivities, and assumptions about the flow convergence around the borehole showed a large variation from extremely low gradients (0.0001 m/m) to—in several cases—seemingly unrealistically high gradients. Most of the calculated gradients were in the interval of 0.01 to 0.1 m/m [22].

These calculated hydraulic gradients are local gradients, which was representative of the naturally flowing fracture(s) in the measured borehole section. However, Nordqvist et al. [22] suggested that, due to various test conditions and interpretation assumptions, these calculated hydraulic gradient values are likely to be too high relative to reasonable topographically-based estimates of the regional hydraulic gradient.

For the purposes of modeling regional flow in the deep crystalline basement, it is necessary to determine a set of parameters (permeability, porosity, and hydraulic head gradient) that produce a representative Darcy velocity (and groundwater pore velocity) for both the intact rock blocks (matrix) and the fracture/fault zones.

A hydraulic head gradient of 0.0001 is assumed for the deep crystalline basement, which is consistent with the lower end of measured values in the Swedish boreholes. A host rock with a matrix permeability of 10^{-18} m^2 and a porosity of 0.005 (Table 1) results in a Darcy velocity of 3×10^{-8} m/yr and a groundwater pore velocity of 0.006 mm/yr.

2.2. Crystalline Basement Fractures

Conceptually, the crystalline host rock is comprised of two entities: matrix and fractures. There are two main approaches for simulating groundwater flow with heat and mass transport in fractured rock: (1) modeling the fluid transport through each individual fracture (i.e., the discrete fracture network (DFN) approach); and (2) modeling the transport regime as an equivalent porous and anisotropic continuum (i.e., the equivalent continuous porous medium (ECPM) approach) [14,17].

A planar fracture is defined by orientation, location, radius, aperture, and transmissivity. DFNs are networks of two-dimensional (2D) fracture planes distributed in a three-dimensional (3D) domain. DFNs are limited by their inability to simulate heat conduction through the rock matrix (and resulting inability to capture the effects of thermally driven fluid fluxes or to couple chemical processes to thermal processes), and by the availability of the computational resources that are necessary to simulate problems involving high fracture density, a large domain size, or multiple unknowns such as, for instance, multiple chemical species. When DFNs become large, simplifications are commonly made, such as modeling flow only in fracture intersections (pipe model); using ECPM representations in all or part of the model domain; breaking the problem into smaller pieces; simulating only steady-state flow regimes; and/or relying on particle tracking instead of solving the set of fully coupled reactive flow and transport equations.

Due to the need to simulate thermally-driven fluid fluxes, the ECPM approach was used to represent the borehole-intersecting fracture in the stuck package scenario. A single, dipping, discrete fracture plane was derived from a DFN based on the fracture system in the well-characterized Forsmark metagranite [23,24]. The fracture plane properties (transmissivity = 1.5×10^{-6} m^2/s, aperture = 1.2×10^{-4} m) were conservatively chosen to create a relatively permeable feature at depth; for example, fracture transmissivity is at the upper end of values derived from packer tests in shallower deformation zones (~500 m) in the Forsmark metagranite [25]. However, it is likely that such a permeable feature intersecting the borehole would be identified during site characterization and/or drilling, and would result in the borehole being abandoned or relocated.

The discrete fracture plane was mapped to the PFLOTRAN porous medium model domain; then, properties for the porous medium grid cells (anisotropic permeability, porosity) intersected by the fracture were calculated from the fracture properties (transmissivity, aperture). The resulting borehole-intersecting fracture in the stuck package scenario consists of a "plane" of ECPM grid cells

15 m on each side, and conceptually can be thought of as equivalent to a 15-m thick brittle deformation zone. The fracture/deformation zone has a dip of 30° and intersects the borehole at a depth of 2540 m.

For the ECPM representation of the "fracture" grid cells, anisotropic permeability depends upon the orientation and transmissivity of the fracture; porosity additionally depends on the fracture aperture. The ECPM anisotropic permeability, as used here, is the permeability in the direction of the fracture (i.e., dipping at 30° relative to the horizontally-oriented PFLOTRAN model domain and grid). This directional permeability is produced in PFLOTRAN by separate permeability values in the x, y, and z grid directions. Transmissivity, T (m²/s), is equivalent to Kb, where K (m/s) is defined by Equation (2) and b (m) is fracture thickness. For $T = 1.5 \times 10^{-6}$ m²/s, $b = 15$ m, fluid (brine) density ≈ 1000 kg/m³, and viscosity $\approx 1 \times 10^{-3}$ Pa·s, the corresponding fracture permeability is 1×10^{-14} m². The discrete fracture location, orientation, transmissivity, and aperture were input to a python script called mapDFN, which calculates ECPM anisotropic permeability by rotating the fracture transmissivity tensor into the coordinates of the grid, and ECPM porosity by dividing the length of the grid cell by fracture aperture [14]. The resulting ECPM fracture properties, anisotropic permeability = 1×10^{-14} m², and porosity = 8.1×10^{-6} were implemented in the PFLOTRAN grid and are summarized in Table 1.

The ECPM fracture porosity, which is several orders of magnitude smaller than the matrix porosity, creates high groundwater pore (linear) velocities that are typical of fracture flow. With a hydraulic head gradient of 0.0001, these fracture properties result in a Darcy velocity and a groundwater pore velocity in the fracture of 2×10^{-4} m/yr and 27 m/yr, respectively.

3. Results for the Nominal Scenario

Nominal scenario PA simulations with PFLOTRAN included a baseline deterministic run [5] and a set of probabilistic realizations (using DAKOTA for Latin hypercube sampling from parameter distributions) to examine the sensitivity and importance of long-term radionuclide transport to selected processes and parameters [5]. The deterministic nominal scenario PA results are summarized here.

The PA model domain for the nominal scenario (Figure 5) is 2D axisymmetric with a radius of 923.627 m and a height of 2534.08 m. The base of the 534.08-m long EZ lies 5000 m below the land surface (mbs); the EZ contains 1084.76-m long WPs and two 10-m long cement plugs. To minimize the peak temperature in the EZ, the cooler Cs WPs are emplaced in the lower portion of the EZ, where the ambient temperature is higher, overlain by the hotter Sr WPs. The EZ liner is not modeled. Instead, the entire annular space between the WPs and the borehole wall DRZ is modeled as a brine-filled EZ annulus.

The PA model for the nominal scenario includes only the lower portion of the SZ, which is a 1000-m interval consisting of alternating lengths of cement, bentonite, and ballast, extending from the top of the uppermost WP in the EZ to the top of the model domain. Two 100-m-long cement plugs sit at the top and bottom of the lower SZ; five additional cement plugs (each 100-m long) separate alternating 50-m lengths of bentonite seal and ballast material. A DRZ that is 0.15 m in width envelopes the entire length of the borehole.

At the time of WP breach (assumed one year after sealing), the entire (decayed) inventory of ^{137}Cs, [135]Cs, and/or ^{90}Sr in a WP is assumed to be present in solution within the WP cell, based on the reference case assumption of unlimited solubility of Cs and Sr in the EZ. The instantaneous dissolution of the entire 18-capsule inventory (in 2050) in a WP into the void space of the WP results in a dissolved concentration (source term) of approximately 0.83 mol/L for Cs (from [135]Cs and ^{137}Cs) and approximately 0.25 mol/L for Sr (from ^{90}Sr). Unlimited solubility for Cs and Sr is also assumed in the PA model domain beyond the EZ.
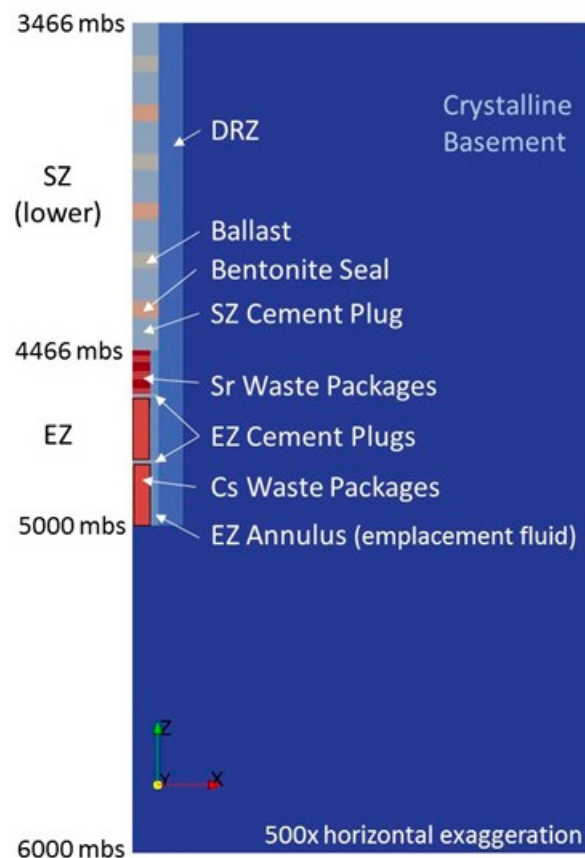
Figure 5. A portion of the DBD PA model domain for the nominal scenario. Source: Freeze et al. [5].

Predicted temperatures, fluid fluxes (specific discharge), and radionuclide concentrations for 10,000,000 years were captured at several observation point depths within the model domain, with a focus on the EZ and lowermost SZ cement plug, including the surrounding DRZ.

Temperatures in the EZ, driven by the heat of radioactive decay, peak at ~3 years, reaching 240 °C near the midpoint of the EZ. This is below the boiling temperature at 5 MPa; hence, there will be no multi-phase flow. The increase in temperature creates a thermally-driven upward fluid flux that includes effects from fluid thermal expansion (early fluxes of very short duration) and buoyant convection (later fluxes due to buoyancy of the hot fluid, which generally peak at the same time as temperatures, and are relevant to possible radionuclide transport) [26]. The buoyancy-driven flux is largest in the brine-filled EZ annulus of the borehole. However, ~25 m above the top of the EZ, buoyancy-driven vertical specific discharge does not exceed 0.0001 m/yr within the lowermost SZ cement plug or 0.006 m/yr within the surrounding DRZ.

Figure 6 shows the concentration of long-lived ^{135}Cs throughout the model domain at 10,000,000 years. The lack of significant buoyancy-driven fluid flux in the SZ is apparent from the negligible ^{135}Cs concentration within the SZ. Even at only ~25 m above the top of the EZ, the concentration of ^{135}Cs never rises above the initial background concentration of 10^{-20} mol/L within the lowermost SZ cement plug or within the surrounding DRZ for the entire simulation duration. Instead, most of the ^{135}Cs remains in the lower part of the EZ, where the 74 WPs containing the Cs capsules were originally emplaced. The effects of the two 10-m long EZ cement plugs (centered at depths of ~4805 mbs and ~4604 mbs) on ^{135}Cs movement are also evident. ^{135}Cs also diffuses laterally through the crystalline host rock away from the EZ. However, after 10,000,000 years, the ^{135}Cs concentration contour of 10^{-15} mol/L has only reached a radius of approximately 20 m beyond the EZ. No ^{135}Cs reaches the biosphere, so there is no dose.
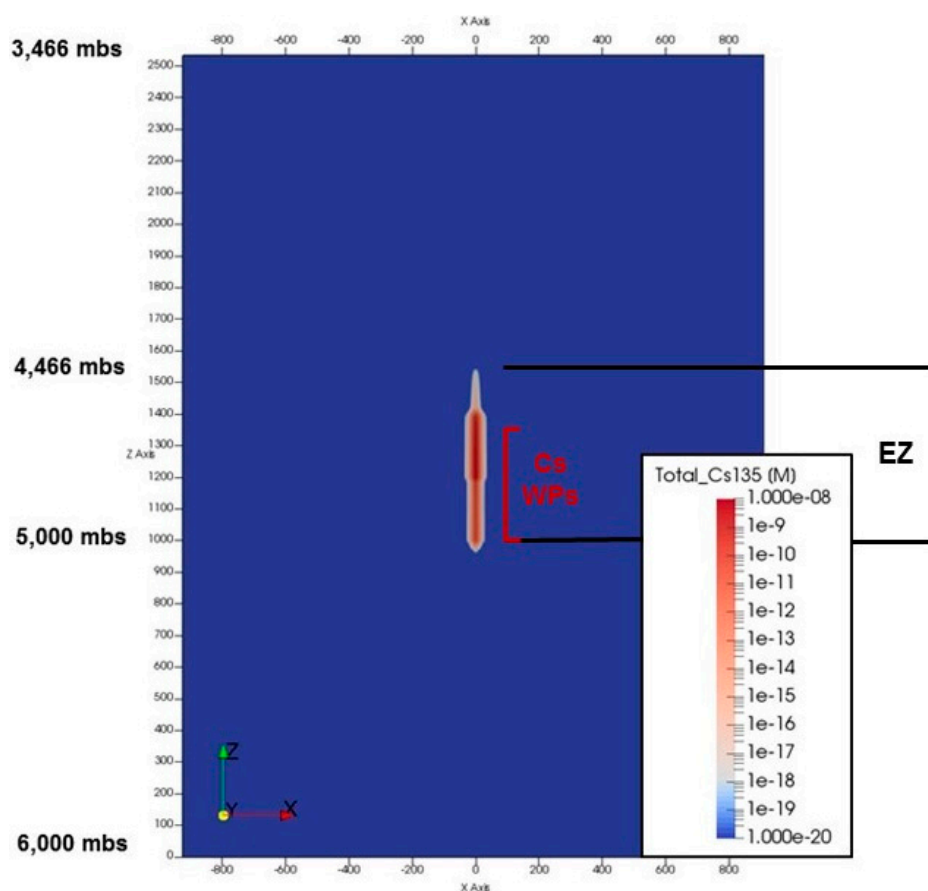
Figure 6. Dissolved concentration of ^{135}Cs at 10,000,000 years for the nominal scenario. Source: Freeze et al. [5].

4. Results for the Stuck Package Scenario

PA simulations with PFLOTRAN for the stuck package scenario included two deterministic runs to examine the sensitivity to the regional head gradient. Otherwise, the stuck package scenario (Figure 7) uses the same reference design, conceptual model, and parameters as the nominal scenario, except for the presence of: (1) a hypothetical borehole-intersecting fracture in the crystalline basement above the EZ, (2) a single Cs WP stuck near the borehole-intersecting fracture, and (3) cement injected into the SZ below the stuck package instead of engineered seals and plugs.

The presence of the fracture/deformation zone necessitated the use of a half-symmetry 3D model domain for the stuck package scenario simulations; the 3D domain is conceptually equivalent to the 2D axisymmetric domain used in the nominal scenario simulations. The 3D model domain is 2000 m in length (x), 1000 m in width (y), and 6000 m in height (z). The half-symmetry (in the y-direction) borehole is centered in x at the front face of the model domain. Refined discretization in x, y, and z at and around the borehole allows the definition of individual WPs (0.11-m radius), the borehole annulus (0.16-m radius), and the DRZ (0.32-m radius). Due to the nature of the vertical refinement at the borehole, it was necessary to choose a single vertical discretization (dz = 5 m) for cells within and around the borehole. As a result, the lengths of cement, bentonite, and ballast regions in the seal (all multiples of five) were identical to lengths in the 2D axisymmetric grid used in the nominal scenario simulations, and WPs were slightly longer (5 m as compared to 4.76 m in the 2D grid). Grid cell dimensions increase away from the borehole to 15 m in the x and y dimensions.
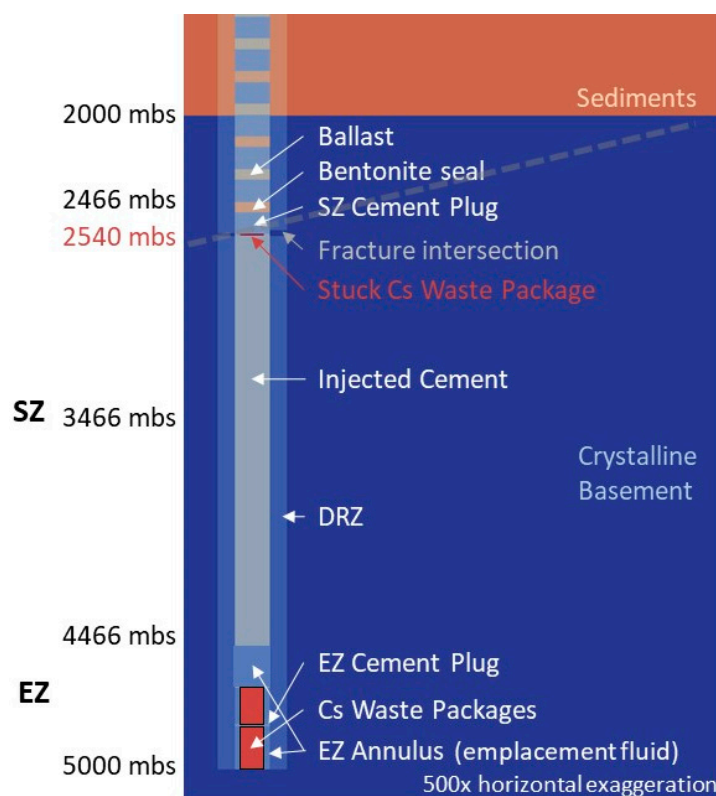
Figure 7. A portion of the DBD PA model domain for the stuck package scenario. Source: Freeze et al. [5].

Whereas the nominal scenario 2D grid had a vertical *z*-dimension of 2534 m (from 6000 m depth to the top of the lower SZ), the stuck package scenario 3D grid has a vertical *z*-dimension of 6000 m (the upper 2000 m consists of undifferentiated sediments; the lower 4000 m form a crystalline basement, including the EZ and SZ). The borehole-intersecting fracture was conceptualized as a 15-m thick brittle deformation zone with a 30° dip that intersects the borehole at a depth of 2540 m and has a permeability of 1×10^{-14} m^2 and a porosity of 8.1×10^{-6}.

For the stuck package scenario, the first 73 Cs WPs are assumed to be emplaced in the lower portion of the EZ, and the final Cs WP is assumed to get stuck in the guidance casing during emplacement at the depth of the fracture intersection (2540 mbs). This location is within the upper SZ, 1926 m above the top of the EZ, and 540 m below the base of the sediments. It is assumed that: (1) the stuck WP cannot be fished, is left in place, and is breached, (2) the SZ seals and plugs below the stuck package are not present, the underlying SZ is instead filled with injected cement to the extent possible (with properties less robust than the engineered cement plugs), and (3) the SZ and UBZ above the stuck WP are sealed and plugged as planned. Due to the stuck package, the 34 Sr WPs are not present.

Deterministic simulations were run with PFLOTRAN for two stuck package scenario cases: one with no regional head gradient, and one with a regional head gradient of 0.0001 m/m, driving flow up-dip toward the base of the sediments. Figure 8 shows the ^{135}Cs concentrations throughout the model domain at 10,000,000 years for each of these cases.

As in the nominal scenario, most of the ^{135}Cs from the first 73 Cs WPs remains in the lower part of the EZ. For the case with no regional head gradient (Figure 8a), a small amount of ^{135}Cs is present in the fracture, due to early-time buoyant convection followed by slow diffusive transport from the single stuck WP. For the case with a regional head gradient of 0.0001 m/m (Figure 8b), ^{135}Cs is advected a distance of approximately 200 m up the fracture over the course of the 10,000,000-year simulation, but is still approximately 400 m below the sediments. This transport distance is consistent with Equation (7), which predicts a center-of-mass transport distance for Cs, with a K_d of 22.5 L/kg, of only 36 m. These preliminary stuck package scenario results suggest that, even in the presence of a regional

head gradient, the long-term advection of radionuclides away from a stuck WP through a hypothetical borehole-intersecting transmissive fracture is minimal. Recall that no performance credit is taken for the WFs or WPs. Robust WFs and/or WPs would further limit and/or delay radionuclide migration.
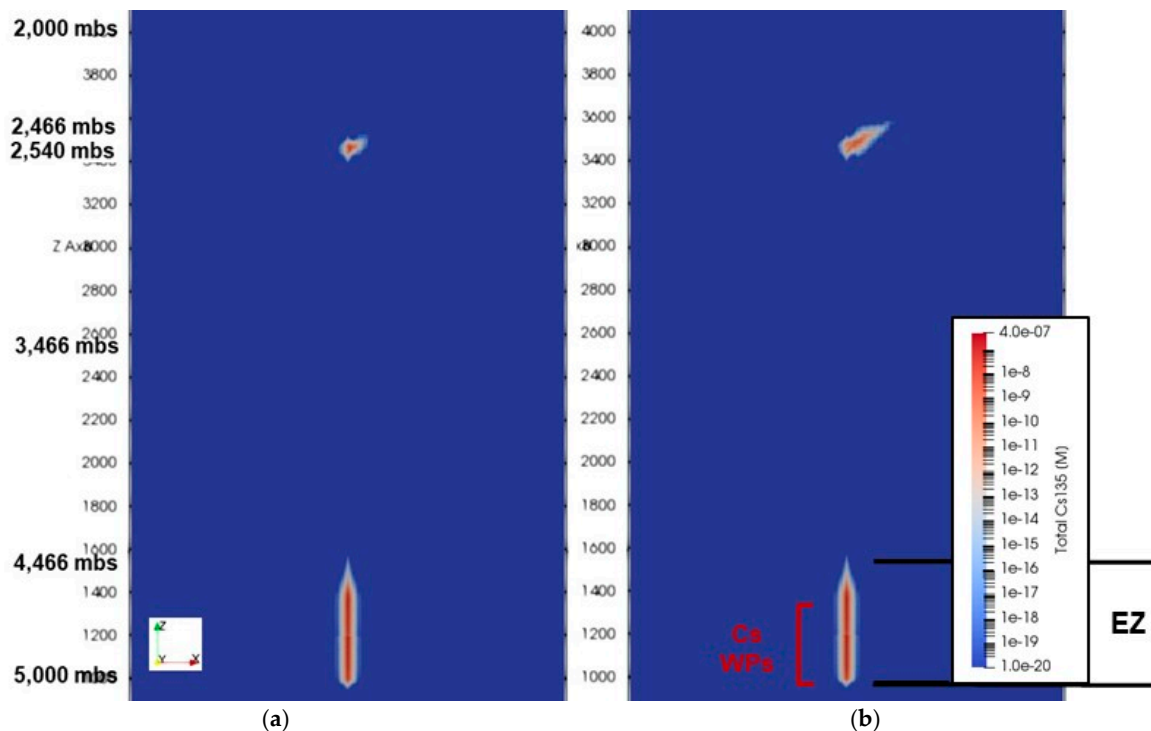

Figure 8. Dissolved concentration of ^{135}Cs at 10,000,000 years for the stuck package scenario. Regional gradient = (**a**) 0 m/m; and (**b**) 0.0001 m/m. Source: Freeze et al. [5].

Author Contributions: Individual contributions include: Conceptualization, G.A.F. and E.S.; Methodology, G.A.F. and E.S.; Formal Analysis, G.A.F. and E.S.; Writing-Review & Editing, P.V.B.

Conflicts of Interest: The authors declare no conflict of interest.

References

1. National Academy of Sciences. *The Disposal of Radioactive Waste on Land*; The National Academies Press: Washington, DC, USA, 1957.
2. Gibb, F.G.F.; Travis, K.P.; Hesketh, K.W. Deep borehole disposal of higher burn up spent nuclear fuels. *Mineral. Mag.* **2012**, *76*, 3003–3017. [CrossRef]
3. Gibb, F.G.F.; Taylor, K.J.; Bukarov, B.E. The 'granite encapsulation' route to the safe disposal of Pu and other actinides. *J. Nucl. Mater.* **2008**, *374*, 364–369. [CrossRef]
4. Gibb, F.G.F. High-temperature, very deep, geological disposal: A safer alternative for high-level radioactive waste. *Waste Manag.* **1999**, *19*, 207–211. [CrossRef]
5. Freeze, G.; Stein, E.; Price, L.; MacKinnon, R.; Tillman, J. *Deep Borehole Disposal Safety Analysis*; FCRD-UFD-2016-000075 Rev. 0, SAND2016-10949R; Sandia National Laboratories: Albuquerque, NM, USA, 2016.
6. Chapman, N.A. Who Might Be Interested in a Deep Borehole Disposal Facility for Their Radioactive Waste? *Energies* **2019**, *12*, 1542. [CrossRef]
7. Holland, G.; Lollar, B.S.; Li, L.; Lacrampe-Couloume, G.; Slater, G.F.; Ballentine, C.J. Deep fracture fluids isolated in the crust since the Precambrian era. *Nature* **2013**, *497*, 357–360. [CrossRef] [PubMed]
8. Gascoyne, M. Hydrogeochemistry, groundwater ages and sources of salts in a granitic batholith on the Canadian Shield, southeastern Manitoba. *Appl. Geochem.* **2004**, *19*, 519–560. [CrossRef]

9.   Park, Y.-J.; Sudicky, E.; Sykes, J. Effects of shield brine on the safe disposal of waste in deep geologic environments. *Adv. Water Resour.* **2009**, *32*, 1352–1358. [CrossRef]

10.   Phillips, S.; Igbene, A.; Fair, J.; Ozbek, H.; Tavana, M. *A Technical Databook for Geothermal Energy Utilization*; Lawrence Berkeley Laboratory, University of California: Berkeley, CA, USA, 1981.

11.   U.S. Department of Energy (DOE). *Assessment of Disposal Options for DOE-Managed High-Level Radioactive Waste and Spent Nuclear Fuel*; Office of Nuclear Energy: Washington, DC, USA, 2014.

12.   Ojovan, M.I.; Guskov, A.V.; Prozorov, L.B.; Arustamov, A.E.; Poluketov, P.P.; Serebryakov, B.B. Safety assessment of bore-hole repositories for sealed radiation sources disposal. *MRS Proc.* **1999**, *608*, 141. [CrossRef]

13.   International Atomic Energy Agency (IAEA). *BOSS: Borehole Disposal of Disused Sealed Sources*; IAEA: Vienna, Austria, 2011.

14.   Mariner, P.E.; Stein, E.R.; Frederick, J.M.; Sevougian, S.D.; Hammond, G.E.; Fascitelli, D.G. *Advances in Geologic Disposal System Modeling and Application to Crystalline Rock*; SAND2016-9610R, FCRD-UFD-2016-000440; Sandia National Laboratories: Albuquerque, NM, USA, 2016.

15.   Lichtner, P.C.; Hammond, G.E. *Quick Reference Guide: PFLOTRAN 2.0 (LA-CC-09-047) Multiphase-Multicomponent-Multiscale Massively Parallel Reactive Transport Code*; DRAFT LA-UR-06-7048; Los Alamos National Laboratory: Los Alamos, NM, USA, 2012.

16.   Freeze, R.A.; Cherry, J.A. *Groundwater*; Prentice-Hall: Englewood Cliffs, NJ, USA, 1979.

17.   Garven, G. Continental Scale Groundwater Flow and Geologic Processes. *Annu. Rev. Earth Planet. Sci.* **1995**, *23*, 89–117. [CrossRef]

18.   Farvolden, R.N.; Pfannkuch, O.; Pearson, R.; Fritz, P. *Region 12, Precambrian Shield. The Geology of North America Vol. O-2, Hydrogeology*; Geological Society of America: Boulder, CO, USA, 1988; pp. 101–114.

19.   Bassett, R.L.; Bentley, M.E. *Deep Brine Aquifers in the Palo Duro Basin: Regional Flow and Geochemical Constraints. Report of Investigations No. 130*; Bureau of Economic Geology, University of Texas at Austin: Austin, TX, USA, 1983.

20.   Lobmeyer, D.H. *Freshwater Heads and Ground-Water Temperatures in Aquifers of the Northern Great Plains in Parts of Montana, North Dakota, South Dakota, and Wyoming*; Professional Paper 1402-D; United States Geological Survey: Washington, DC, USA, 1985.

21.   Downey, J.S.; Dinwiddie, G.A. *The Regional Aquifer System Underlying the Northern Great Plains in Parts of Montana, North Dakota, South Dakota, and Wyoming—Summary*; Professional Paper 1402-A; United States Geological Survey: Washington, DC, USA, 1988.

22.   Nordqvist, R.; Gustaffson, E.; Andersson, P.; Thur, P. *Groundwater Flow and Hydraulic Gradients in Fractures and Fracture Zones at Forsmark and Oskarshamn*; Svensk Kärnbränslehantering AB: Stockholm, Sweden, 2008.

23.   Joyce, S.; Harley, L.; Applegate, D.; Hoek, J.; Jackson, P. Multi-Scale Groundwater Flow Modeling During Temperate Climate Conditions for the Safety Assessment of the Proposed High-Level Nuclear Waste Repository Site at Forsmark, Sweden. *Hydrogeol. J.* **2014**, *22*, 1233–1249. [CrossRef]

24.   Follin, S.J.; Hartley, L.; Rhen, I.; Jackson, P.; Joyce, S.; Roberts, D.; Swift, B. A methodology to constrain the parameters of a hydrogeological discrete fracture network model for sparsely fractured crystalline rock, exemplified by data from the proposed high-level nuclear waste repository site at Forsmark, Sweden. *Hydrogeol. J.* **2014**, *22*, 313–331. [CrossRef]

25.   Follin, S.J.; Levén, J.; Hartley, L.; Jackson, P.; Joyce, S.; Roberts, D.; Swift, B. *Hydrogeological Characterization and Modelling of Deformation Zones and Fracture Domains, Forsmark Modelling Stage 2.2. SKB R-07-48*; Svensk Kärnbränslehantering AB: Stockholm, Sweden, 2007.

26.   Sandia National Laboratories (SNL). *Deep Borehole Field Test Conceptual Design Report*; FCRD-UFD-2016-000070, Rev. 1, SAND2016-10246R; SNL: Albuquerque, NM, USA, 2016.